Rapid Voltage Change Detection: Limits of the IEC Standard Approach and Possible Solutions

David Macii, *Senior Member, IEEE*, Dario Petri, *Fellow, IEEE*
Department of Industrial Engineering
University of Trento
Trento, Italy
david.macii@unitn.it

***Abstract* – Rapid Voltage Changes (RVCs) are Power Quality (PQ) events characterized by small and fast transitions between two steady-state Root Mean Square (RMS) voltage levels. RVCs occur quite often at the distribution level and are expected to be even more frequent in the future due to the increasing penetration of dynamic loads and renewable-based generators in the smart grid. Unlike other PQ events, RVCs are less critical, but also more difficult to detect than dips/sags and swells, due to their smaller voltage variations. Nevertheless, they can be harmful for generators control systems and electronic equipment in general. Moreover, they strongly affect flicker. The IEC Standard 61000-4-3:2015 clearly describes an algorithm for RVC detection. However, this approach is poorly characterized in the scientific literature. In fact, it suffers from some drawbacks. In this paper, some of them (e.g. rate-dependent detection limits and detection delays) are analyzed in depth. In addition, an alternative approach based on the estimation of the rate of change of RMS voltage is proposed. Multiple simulation results show that the approach considered is more sensitive to noise, but also faster, especially when not so fast RVCs occur. Moreover, it allows to measure the rate of change of RMS voltage, which is currently disregarded in the IEC Standard.**

***Keywords* – Power quality, Rapid Voltage Changes (RVCs), signal processing, smart grid, estimation uncertainty.**

I. INTRODUCTION

Rapid Voltage Changes (RVCs) are sudden voltage fluctuations, which are not so large to be regarded as dips/sags or swells, but that, nonetheless, may strongly affect Power Quality (PQ) and particularly flicker [1], [2]. Furthermore, RVCs may cause control system malfunction or could jeopardize the correct operation of electronic equipment [3].

Generally, RVCs arise from switching operations, e.g. due to motor starting, capacitor banks switching, fast load/generation variations or transformer tap changes. Even if RVCs have been recognized as a potential cause of PQ issues for many years [4], the need to detect them and to measure their properties has been acknowledged only quite recently as a result of the increasing penetration of distributed energy resources (such as photovoltaic or wind power systems) in the context of smart grids [5]. Even if the IEEE Standard 1159-2009 on PQ monitoring does not provide any RVC definition [6], the Technical Committee revising the IEEE Standard 1159.3-2003 on Power Quality Data Interchange Format (PQDIF) is currently discussing about the possibility to classify and to report RVCs in a vendor-independent manner [7], thus addressing the needs highlighted by both the IEC Technical Committee 85 and the Norwegian regulator [8]. The IEC Standard 61000-4-30:2015 defines an RVC as "a quick transition in Root Mean Square (RMS) voltage between two steady-state conditions, during which the voltage does not exceed the dip/swell thresholds" [9].

While the measurement problems associated with other PQ phenomena such as flicker [10], [11], [12], harmonics and interharmonics [13], [14], or voltage dips/sags and swells [15], [16], [17], have been already analyzed in depth over the last 20 years, till now RVCs have received little attention from the scientific community due to their lower impact on PQ. As a consequence, RVC detection and measurement techniques are still poorly characterized from the metrological viewpoint. However, the recent, increasing probability to incur voltage fluctuations in smart grids is currently changing this attitude.

An overview of some typical RVC models (i.e. step-like events, linear ramps or motor start-up) as well as an analysis of the effect of different types of RVCs on the PQ perceived by users is presented in [8]. However, that work is focused on the minimum requirements for RVC monitoring and does not suggest any specific detection technique. A well-established RVC detection algorithm is instead described in the IEC Standard 61000-4-30:2015 [9]. The core of this algorithm simply relies on the comparison between the most recent 100 or 120 RMS voltage values (for 50 Hz or 60 Hz systems, respectively) estimated over one-cycle-long intervals and refreshed every half-cycle, and the corresponding moving average computed over the last second. In particular, if the absolute value of the difference between such RMS voltage estimates and the corresponding moving average exceeds the moving average itself by a few percent, the collected voltage waveform is considered to be no longer in steady state. In this case (and if the dip/sag or swell thresholds are not exceeded in the meanwhile), an RVC is detected. Afterwards, the RVC detection thresholds could be optionally and temporarily decreased by a specified amount to introduce a hysteresis reducing the probability that repeated threshold crossings may wrongly lead to multiple RVC detections associated with the same event [9].

Unfortunately, the IEC Standard algorithm briefly summarized above suffers from various limitations, e.g., absence of univocal criteria to set the detection and hysteresis

thresholds, missing specifications about the minimum aggregation time needed to consider successive RVCs as separate events, and above all, unconcern about the influence that the rate of change of RMS voltage can have on RVC detection [18]. In fact, it was observed through simulations that using the moving average to set the RVC detection thresholds may cause significant delays, when the RVCs are not particularly fast [19]. Thus, the primary goal of this paper is to investigate in depth the effect of the rate of change of RMS voltage on RVC detection, in order to propose possible alternative solutions. In particular, in Section II it will be shown analytically that both the ability of the IEC Standard algorithm to detect an RVC and the respective detection delays depend not only on the RMS voltage levels and the corresponding thresholds, but also on the rate of change of RMS voltage. This behavior is inherently due to the use of time-varying detection thresholds (i.e., based on the moving average), regardless of the specific RMS estimators adopted. Therefore, even though alternative RMS voltage estimators (e.g. relying on the Taylor's series of the fundamental phasor as suggested in [19]), tend to react more promptly to possible voltage variations (especially in the presence of step-like changes [20]), the underlying general detection limitations of the IEC Standard algorithm still persist. For the same reason, even if adapting existing phasor estimation algorithms to PQ monitoring problems can speed up event detection [21], [22], [23], the analysis of RVCs based on Phasor Measurement Units (PMU) suffers from various drawbacks [24]. Of course, RVC detection results can be also affected by measurement uncertainty, since not only the individual RMS voltage values, but also the detection thresholds depend on measurement data [25]. A thorough analysis of the impact of sudden voltage amplitude and phase changes on the accuracy of the RMS estimator adopted by the IEC Standard algorithm is presented in [26]. However, that analysis does not take into consideration the effect of measurement uncertainty in the case of smooth RVCs, nor its influence on the detection thresholds. These issues are instead investigated in Section II.C.

For all the reasons above, in Section III a completely different and novel RVC detection approach (i.e., based on the estimation of the rate of change of RMS voltage instead of the RMS voltage) is proposed. The key advantages of this approach are: higher detection speed (especially when RVCs are not particularly fast) and the ability to measure the rate of change of RMS voltage.

Its main drawback is instead the higher sensitivity to random uncertainty contributions. In fact, the threshold on rate of change of RMS voltage cannot be lower than a few %/s; otherwise the risk of false detection might become excessively large. This will be shown in Section IV where the performances of the standard and the alternative RVC detection algorithms are compared in realistic conditions. The main conclusions of the paper and an outline of future work will be finally reported in Section V.

II. Theoretical Analysis of RVC Detection Based on the Algorithm of IEC Standard IEC 61000-4-30:2015

To a first approximation, a single-phase AC voltage waveform affected by a linear-ramp RVC can be modeled as [8]

$$x(t)=\begin{cases} U\,\boldsymbol{sin}(2\pi ft+\varphi) & t\le t^* \\ U\left[1+R\left(t-t^*\right)\right]\boldsymbol{sin}(2\pi ft+\varphi) & t>t^* \text{ and } t\le t^*+T_R \\ U\left[1+\delta_U\right]\boldsymbol{sin}(2\pi ft+\varphi) & t>t^*+T_R \end{cases} \quad (1)$$

where symbols U, f and φ represent the amplitude, the fundamental frequency, and the initial phase, respectively, of the collected waveform, R is the rate of change of RMS voltage, t^* is the time when the RVC begins, T_R is the RVC duration, δ_U is the voltage relative amplitude variation once the new steady state is reached. Even if model (1) is quite simple and it does not include noise or harmonic/interharmonic disturbances (which instead will be considered in the simulation-based analysis described in Section IV), it is general enough to perform a quite in-depth performance analysis of the detection mechanism based on the algorithm reported in the IEC Standard 61000-4-30:2015 [9]. Moreover, (1) includes the classic step-like model as a special case, provided that R is large enough.

In [9], the RMS voltage values of the collected waveform are estimated over subsequent overlapped one-cycle-long intervals (starting/ending at a zero crossing) and refreshed every half-cycle. Let $U_{rms(1/2)}(i)$ be the RMS voltage at the end of the i-th half-cycle. If all temporal quantities are discretized with period $T/2$ (where $T=1/f$), time variable t^* in (1) can be expressed as $t^* = L\cdot T/2 + \tau$, where L is an integer number and τ is a random variable uniformly distributed in [0, $T/2$] since an RVC may occur at any time within a half-cycle. Similarly, the RVC duration can be expressed as $T_R = K\cdot T/2 + \tau_R$ where K is an integer number. Since not only the beginning, but also the end of an RVC may occur randomly during a power line half-cycle, and considering that these two events can be assumed to be independent, τ_R exhibits a triangular distribution within [-$T/2$, $T/2$]. If N is the number of RMS values estimated in 1 second (i.e. $N = 2/T$, with T expressed in seconds), and $\overline{U}_{rms(1/2)}(i)$ is the corresponding moving average, a voltage waveform is supposed to be no longer in steady-state (i.e., an RVC is detected) as soon as $\exists\, i^*$ such that for $i^*\le i<i+N$

$$\left|U_{rms(1/2)}(i)-\overline{U}_{rms(1/2)}(i)\right| \ge S\cdot\overline{U}_{rms(1/2)}(i) \quad (2)$$

where S is a given small, but positive value, usually ranging between 1% and 6% [9]. However, thresholds even lower than 1% could be needed to analyze the relationship between RVCs and flicker [1], [8]. Of course, in general (2) can be affected by various uncertainty contributions. In the following subsections, first the theoretical limits for RVC detection using the IEC Standard algorithm in ideal conditions (i.e., when measurement uncertainty is negligible) and the related

maximum detection delays will be determined. Then, the effect of measurement uncertainty will be analyzed.

A. RMS voltage rate of change limits for RVC detection

The moving average operator used to set the thresholds for RVC detection acts as a low-pass filter. Therefore, the rate of change of $\overline{U}_{rms(1/2)}(i)$ (either positive or negative) is certainly lower than the rate of change of individual RMS voltage variations. As a consequence, the difference $\left|U_{rms(1/2)}(i)-\overline{U}_{rms(1/2)}(i)\right|$ in (2) is maximum for $i = L+K$, i.e. as soon as the voltage signal (1) reaches a new steady-state. Afterwards, for $i > L+K$, $\left|U_{rms(1/2)}(i)-\overline{U}_{rms(1/2)}(i)\right|$ starts decreasing and it tends ideally to zero when also $\overline{U}_{rms(1/2)}(i)$ reaches the new steady state level. Therefore, if condition (2) is not met for $i = L+K$, certainly an RVC described by model (1) will not be detected. This qualitative analysis suggests that for given values of parameters δ_U and S, a critical rate of change of RMS voltage exists below which RVCs cannot be detected. An example of an undetected RVC is clearly visible in Fig. 1(a) which depicts the RMS voltage values of (1) (assuming, for example, a Signal-to-Noise Ratio of 60 dB) along with the corresponding upper and lower detection thresholds (dotted lines) based on (2) for S=5%, when an RVC with R = -5 %/s and δ_U = -10% occurs. Fig. 1(b) shows a dual example when an RVC with the same amplitude variation (i.e., δ_U = -10%), but a higher, negative rate of change of RMS voltage (i.e., R = -20 %/s) is instead detected. Thus, the ideal limit of the rate of change of RMS voltage for RVC detection is the value of R for which condition (2) turns approximately into an equation, i.e. for $i = i^* = L+K$.

In Appendix A the general analytical of $\overline{U}_{rms(1/2)}(i)$ (expression (A.4) is reported. In particular, for $i^* = L+K$, (A.4) becomes

$$\overline{U}_{rms(1/2)}(L+K)=\frac{U}{\sqrt{2}}\left\{1+\frac{RT}{4N}K(K-1)+\frac{K}{N}R\tau_R\right\}. \quad (3)$$

Assuming that $|\delta_U| \geq S$ (which is a necessary condition for correct RVC detection), it is shown in Appendix B that, if T is expressed in seconds, by replacing first $K=\frac{2\delta_U}{RT}-\frac{2\tau_R}{T}$ into (3), and then (3) and $U_{rms(1/2)}(L+K)\cong U(1+\delta_U)$ into (2), after some algebraic steps the following conditions on the rate of change of RMS voltage for RVC detection result, i.e.

$$R > R_{m+} \approx \frac{2\delta_U}{T+\frac{4}{1+S}\left(1-\frac{S}{\delta_U}\right)} > 0 \quad (4)$$

for positive RVC (i.e. for δ_U>0) and

$$R < R_{m-} \approx \frac{2\delta_U}{T+\frac{4}{1-S}\left(1+\frac{S}{\delta_U}\right)} < 0 \quad (5)$$

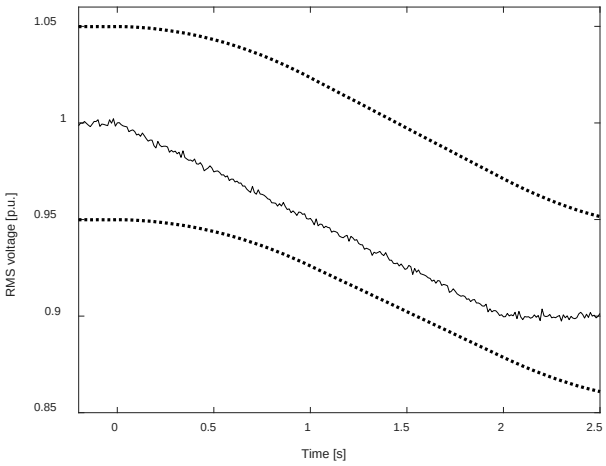

(a)

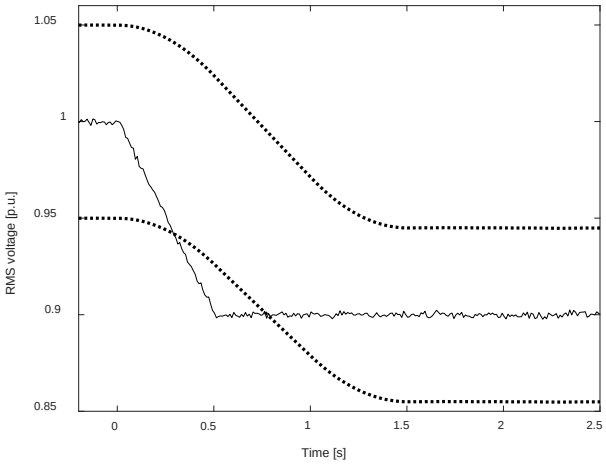

(b)

Fig. 1 – RMS voltage values during two different RVCs (solid lines) when the upper/lower detection thresholds based on the IEC Standard 61000-4-15 are computed assuming S=5% (thick dotted lines). In both cases, the relative amplitude variation is the same (i.e. δ_U = -10%), but the rate of change is different, i.e. R = -5 %/s in (a) and R = -20 %/s in (b). In (a) the estimated RMS value does not reach the threshold and so the RVC is not detected.

for negative RVC (i.e. if $\delta_U < 0$), respectively. Note that $|R_{m+}| \neq |R_{m-}|$. Therefore, the ability of the IEC Standard algorithm to detect positive and negative RVCs is not exactly the same. In particular, if $|\delta_U| >> S$, R_{m+} and R_{m-} become very small as they tend asymptotically to $\delta_U/2$. On the contrary, when $|\delta_U|$ approaches S, R_{m+} and R_{m-} grow sharply till reaching $\frac{2\delta_U}{T}$. Observe also that R_{m+} and R_{m-} represent the safe limits of the rate of change of RMS voltage for which the IEC standard algorithm is able to detect RVCs. This means that if conditions (4) or (5) hold true, RVCs with RMS voltage increasing or decreasing linearly shall be certainly detected. If instead $R_{m-} < R < R_{m+}$, RVCs are hardly recognizable, but they could be sporadically detected in any case for "lucky" values of τ_R or φ, or simply as a result of the

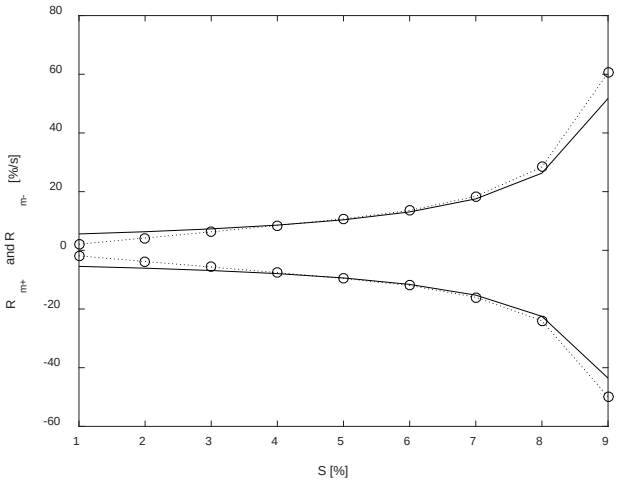

Fig. 2 – Minimum positive and maximum negative rates of change of voltage for which an RVC is detected. The solid lines refer to the approximate analytical results given by (4) and (5) for T = 20 ms and δ_U=±10%, whereas the dotted lines with markers are obtained through simulations.

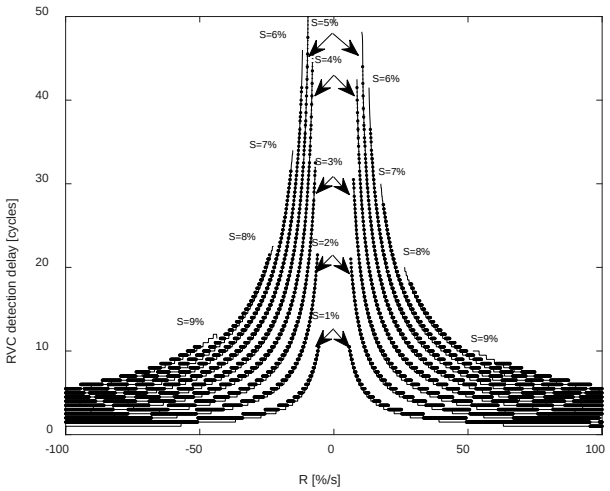

Fig. 3 – Maximum RVC detection delays as a function of positive and negative rates of change of RMS voltage for different values of the relative detection threshold S. In all cases T = 20 ms and δ_U = ±10%. The solid lines are based on (6), while the dotted lines result from Monte Carlo simulations.

overshoots/undershoots affecting RMS voltage estimation, as it may happen if significant phase jumps occur [26].

In practice, the typical range of voltage relative amplitude variations for which an RVC should be certainly detected is $1\% \leq |\delta_U| < 10\%$ [1].

To check the correctness of the proposed analysis, the values of R_{m+} and R_{m-} given by (4) and (5) are compared with the results of Monte Carlo simulations obtained by using 50-Hz waveforms (i.e. T = 20 ms) with $U/\sqrt{2}$ = 1 p.u. and δ_U = ±10%. In every simulation, the rate of change R (initially set to ±1 %/s) is increased or decreased linearly by steps of 0.1 %/s for different values of S till when an RVC is detected. Moreover, 50 values of variables φ and t^* in (1) are changed randomly with a uniform probability density function within $[0,2\pi]$ and $[1, 1+T/2]$ seconds, respectively. Once the 50 positive or negative values of R associated with the first RVC detection are found, the respective maximum and minimum are computed. Such values provide a numerical estimate of R_{m+} and R_{m-}, respectively. Fig. 2 shows the values of R_{m+} and R_{m-} obtained from (4) and (5) (solid lines) and based on simulations (dotted lines with circle markers), respectively, for S ranging between 1% and 9% (greater values of S are not considered in the present analysis, because thresholds equal to ±10% of the rated RMS voltage are generally used for sags/dips and swells detection). Observe that theoretical and simulation-based results are in good accordance, although they slightly differ for small values of S and when δ_U and S become comparable. Such differences are mainly due to the assumptions made in Appendix B to obtain straightforward and easy-to-use expressions for R_{m+} and R_{m-}. However, the small difference between the simulation results and those based on (4) and (5) confirm that the assumptions underlying the approximate expressions are sound.

The experimental data reported in [1] and collected in a low-voltage distribution system show that, for S=1%, the absolute values of the rates of change of RMS voltage associated with the smoother RVCs can be well below 75 V/s (i.e. lower than 32%/s for 230 V_{RMS} systems). However, no clear lower bounds are reported. Expressions (4) and (5) confirm instead that events with a rate of change so small as about 5 %/s can be detected.

It is interesting to note that if the declared RMS voltage value $U/\sqrt{2}$ instead of $\overline{U}_{rms(1/2)}(i)$ were used in (2), possible RVCs would be detected for any value of R, provided that $|\delta_U| > S$. In fact, the choice of referring the upper and lower threshold for RVC detection to the moving average of the last N RMS estimates enables RVC detection even when the steady-state RMS voltage differs from the nominal value, e.g., due to given load conditions. On the other hand, the ability of the IEC algorithm to detect an RVC clearly depends on the rate of change of RMS voltage as well. In particular, by increasing S, the chance to detect not only small events, but also RVCs, which are not particularly fast, tends to diminish drastically, especially when $|\delta_U|$ tends to S.

B. RVC detection delay using the IEC Standard algorithm

The RVC example plotted in Fig. 1(b) shows that when an RVC is detected, the upper or lower threshold is generally crossed twice. The RVC detection delay can be defined as the time interval between the instant when an RVC actually begins and the instant (corresponding to an integer multiple of a half power-line cycle) when one of the detection thresholds is crossed for the first time.

A closed-form expression of the RVC detection delay can be derived by finding the minimum number of half-cycles $D=i^*-L \leq K \leq N-1$, for which (2) is satisfied. In particular, it is shown in Appendix C that the worst-case RVC detection delay expressed in half-cycles is given by

$$D_{max} \approx \begin{cases} \left\lceil \left| \dfrac{2}{T(1+S)} \left(1 - \sqrt{1 - 2(1+S)\left(\dfrac{S}{R} - \dfrac{T}{2}\right)} \right) \right| \right\rceil & R \geq R_{m+} \\ \left\lceil \left| \dfrac{2}{T(1-S)} \left(1 - \sqrt{1 + 2(1-S)\left(\dfrac{S}{R} + \dfrac{T}{2}\right)} \right) \right| \right\rceil & R \leq R_{m-} \end{cases} \quad (6)$$

where function $\lceil \bullet \rceil$ rounds its argument to the closest larger integer value. Observe that if $|R| \geq \frac{2S}{T}$ (which is typically much larger than $|R_{m+}|$ or $|R_{m-}|$) an RVC is certainly detected within the first half-cycle. In this case (6) tends to converge to 1.

Again, the validity and accuracy of (6) have been checked through Monte Carlo simulations in the very same conditions as those described in Section II.A. Fig. 3 shows the analytical and simulated values of D_{max} as a function of both positive and negative rates of change of RMS voltage when $\delta_U = \pm 10\%$ and for S ranging between 1% and 9%. The solid lines refer to the results returned by (6), whereas the dotted lines are obtained through simulations by computing the maximum detection delays over 50 trials for different values of φ and t^*. Observe that, in this case, analytical and simulation-based results match almost perfectly. The slight asymmetry of the curves is due to the different expressions in (6), when positive and negative RVCs are considered. It is also worth noting that, when $|R|$ is below a given threshold, RVC detection becomes infeasible, in accordance with the analysis reported in Section II.A. Moreover, if S and $|\delta_U|$ get closer, the RVC detection delay tends to grow quickly. Even though this result is quite intuitive, the curves in Fig. 3 show that the relationship between detection delay, rate of change of RMS voltage and detection thresholds is strongly nonlinear. In particular, when $|R| \leq 50$ %/s, the worst-case detection delays can be in the order of tens of cycles. This does not sound very reasonable since "rapid" events are supposed to be detected quickly.

C. Influence of measurement uncertainty on RVC detection using the IEC Standard algorithm

The analysis in Section II.A highlights that by decreasing the relative threshold S, the standard algorithm is able to detect not only smaller voltage changes, as expected intuitively, but also RVCs with a lower rate of change of RMS voltage, since $|R_{m+}|$ and $|R_{m-}|$ increase monotonically with S. However, till now the effect of measurement uncertainty on RVC detection has not been taken into account. As known, measurement uncertainty is mainly due to:

- possible systematic deviations introduced by the measuring equipment;
- random contributions due to the cascade of transducers, data acquisition circuitry and acquisition jitter (including the jitter associated with zero-crossing detection) [27].

The joint effect of all such contributions can be modelled by a single additive random process $\eta(\cdot)$. To a first approximation, this process can be assumed to be wide-sense stationary and normally distributed, with mean value μ_η and variance σ_η^2, where $\mu_\eta \neq 0$ is mainly due to systematic deviations, whereas σ_η depends only on the random contributions and includes the joint effect of both voltage fluctuations and jitter, as explained in [28]. It is important to highlight that $\eta(\cdot)$ does not affect RVC detection directly, but through the classic one-cycle RMS voltage estimator defined in the IEC Standard [9], i.e.

$$\hat{U}_{rms(1/2)}(i) = \sqrt{\frac{1}{M}\sum_{m=0}^{M-1}\left[x\left(i\frac{T}{2} - mT_s \right) + \eta\left(i\frac{T}{2} - mT_s \right)\right]^2} \quad (7)$$

where index i refers to the i-th half-cycle, $x(\cdot)$ is given by (1), T_s is the sampling period of the measurement instrument and M is the number of samples in one nominal power line cycle. Of course, (7) can be more compactly rewritten as $\hat{U}_{rms(1/2)}(i) = U_{rms(1/2)}(i) + \varepsilon(i)$. Since $\eta(\cdot) << x(\cdot)$ is normally distributed and recalling that the fourth-order central moment of a normal random variable is $3\sigma_\eta^4$, by following an approach similar to the one described in [29], it can be shown that the mean value and the variance of $\varepsilon(\cdot)$ are

$$\mu_\varepsilon \approx \frac{\mu_\eta^2 + \sigma_\eta^2}{2U_{rms}} \quad \text{and} \quad \sigma_\varepsilon^2 \approx \frac{\sigma_\eta^2}{M} + \left(1 + \frac{2}{M}\right)\frac{\sigma_\eta^4}{4U_{rms}^2} \approx \frac{\sigma_\eta^2}{M}, \quad (8)$$

respectively. If $\hat{\bar{U}}_{rms(1/2)}(i) = \bar{U}_{rms(1/2)}(i) + \bar{\varepsilon}(i)$ denotes the moving average of the last N estimated RMS voltage values and $\bar{\varepsilon}(i)$ is the arithmetic average of the corresponding uncertainty contributions, by replacing $\hat{U}_{rms(1/2)}(i^*)$ and $\hat{\bar{U}}_{rms(1/2)}(i^*)$ at the end of cycle i^* (i.e. when an RVC is detected) into (2), it is evident that, unlike the ideal case, the actual detection threshold is affected by systematic and/or random deviations given by

$$\delta_S(i^*) = \frac{\bar{\varepsilon}(i^*)(1 \pm S) - \varepsilon(i^*)}{U_{rms(1/2)}(i^*)} \quad (9)$$

where $U_{rms(1/2)}(i^*)$ is the RMS voltage when an RVC is supposed to be detected in ideal conditions. Consider that, by definition of RVCs, $U_{rms(1/2)}(i^*)$ is supposed to fluctuate at most by ±10% depending on RVC amplitude and rate of change. Therefore, to a first approximation, the denominator of (9) can be assumed to be almost constant, i.e., $U_{rms(1/2)}(i^*) \approx U_{rms} \approx U/\sqrt{2}$.

Observe that, since the mean values of $\bar{\varepsilon}(\cdot)$ and $\varepsilon(\cdot)$ are the same, the expectation of (9) is

$$E\left\{\delta_S(i^*)\right\} \approx \pm\frac{\sqrt{2}S\mu_\varepsilon}{U} \approx \pm S\frac{\mu_\eta^2 + \sigma_\eta^2}{U^2}. \quad (10)$$

As known, the IEC Standard 61000-4-30:2015 prescribes that instrumental accuracy lies within ±0.2% of the measured RMS voltage for *Class A* equipment and ±1% for *Class S* equipment, respectively. Therefore, the ratio $\frac{\mu_\eta^2}{U^2}$ is certainly smaller than 10^{-4}. Moreover, the total Signal-to-Noise Ratio (SNR) $\frac{U^2}{2\sigma_\eta^2}$ due to the superimposition of multiple independent random contributions is likely to be in the order of 30-60 dB [30]. Therefore, recalling that S is typically lower

than 6% [9], the impact of both instrumental systematic deviations and the bias of (7) on the actual RVC detection thresholds is negligible.

On the other hand, since the variance of $\bar{\varepsilon}(\cdot)$ is $(2N\text{-}1)\sigma_\varepsilon^2/N^2 \approx 2\sigma_\varepsilon^2/N$ and considering that pairs of subsequent values of $\varepsilon(\cdot)$ (i.e., $\varepsilon(i)$ and $\varepsilon(i\text{-}1)$ for any i) are correlated with a correlation coefficient equal to 0.5 (subsequent one-cycle RMS voltage estimates are indeed computed over intervals overlapped by one half-cycle), the variance of (9) for $S<<N$ is

$$\boldsymbol{var}\left\{\delta_S\left(i^*\right)\right\} \approx \frac{2\sigma_\varepsilon^2}{U^2}\left(1-\frac{2}{N}\right) \approx \frac{2\sigma_\eta^2}{MU^2}\left(1-\frac{2}{N}\right). \quad (11)$$

Thus, assuming that the sampling frequency is in the order of some kHz (e.g., M is in the order of 100 samples), the square root of (11) ranges from about 0.01% when SNR= 60 dB to 0.3% when SNR = 30 dB. Therefore, since the average value of the detection threshold deviations is almost null, in order to minimize the risk that possible random fluctuations may cause false RVC detections, the value of S should be much higher than the square root of (11), i.e. in the order of 1%, in accordance with the smallest values proposed in [9]. Moreover, the results of Section II.A suggest that, as a rule of thumb, values of S > 2% should be generally avoided, because not only events with $|\delta_U|$ in the order of 1% would be missed, but also RVCs with relative amplitude variation a bit larger than 2% and absolute rates of change lower than the limits given by (4) and (5) could be hardly detected.

III. RVC Detection based on rate of change of RMS voltage estimation

The analysis reported in Section II paves the way to an alternative and potentially more effective approach for RVC detection based on the comparison between the rate of change of RMS voltage (denoted in the following as U'_{RMS}) and the corresponding threshold R^*. The steps of this alternative RVC detection algorithm are quite simple and are quickly summarized below.

1. The rate of change of RMS voltage at the end of the i-th half-cycle is estimated through the Euler backward difference $\hat{U}'_{rms(1/2)}(i) = 2\frac{\hat{U}_{rms(1/2)}(i)-\hat{U}_{rms(1/2)}(i-1)}{T}$.
2. As soon as $\left|\hat{U}'_{rms(1/2)}\left(i^*\right)\right| \geq \left|R^*\right|$ after cycle i^*, then the waveform is considered to be no longer in steady-state and the logic signal defined in the IEC Standard 61000-4-15:2015 is set to false. Since, in stationary conditions, $\hat{U}'_{rms(1/2)}(i)$ should be ideally null, regardless of the load condition, the use of the moving average for threshold setting is unnecessary in this case.
3. The estimated RMS voltage values $\hat{U}_{rms(1/2)}(i)$ for $i^* \geq i$ are then compared with the limits for dips/sags or swell detection.
4. If such limits are not exceeded, the corresponding event is classified as an RVC and the steady-state logic signal is disabled for at least N half-cycles. The detected RVC is supposed to be over after the i-th half-cycle if $|\hat{U}'_{rms(1/2)}(n)| < \left|R^*\right|$ for $i\text{-}N\text{+}1 \leq n \leq i$. Optionally, the upper and lower thresholds during the 1-second time interval following RVC detection can be decreased by a specified amount to reduce the risk of wrongly detecting the end of the RVC, thus introducing a possible hysteresis, like in the IEC standard algorithm [9]. However, this option is unnecessary for the purposes of the presented analysis and therefore it will not be considered in the rest of this paper.

It is worth emphasizing that this alternative RVC detection algorithm has some potential benefits compared with the standard one. First of all, since the rate of change of RMS voltage is the key parameter identifying a possible non-stationary condition, the derivative-based approach enables a faster detection of RVCs, as it will be shown in Section IV. Secondly, unlike the standard algorithm, the detection limits of the derivative-based approach depend only on the rate of change of the RMS voltage.

A. Influence of measurement uncertainty on RVC detection based on the proposed algorithm

With reference to the same notation and assumptions adopted in Section II.C, the actual detection threshold of the rate of change of RMS voltage at the end of cycle i^* is affected by deviations that can be modeled by variable

$$\delta_R\left(i^*\right) = \frac{2}{T}\frac{\varepsilon\left(i^*\right)-\varepsilon\left(i^*-1\right)}{U_{rms(1/2)}\left(i^*\right)} \approx \frac{2\sqrt{2}}{T}\frac{\varepsilon\left(i^*\right)-\varepsilon\left(i^*-1\right)}{U}. \quad (12)$$

Observe that the systematic contributions affecting individual one-cycle RMS voltage estimates tend to be cancelled by the backward Euler difference. Therefore, again their impact on (12) is negligible. On the contrary, since variables $\varepsilon(i)$ and $\varepsilon(i\text{-}1)$ are correlated with a correlation coefficient equal to 0.5 for the same reasons explained in Section II.C, the variance of (12) due to the random uncertainty contributions is

$$\boldsymbol{var}\left\{\delta_R^2\right\} = \frac{8\sigma_\varepsilon^2}{T^2 \cdot U^2} \approx \frac{8}{T^2 \cdot U^2}\frac{\sigma_\eta^2}{M}. \quad (13)$$

Again, the approximate rightmost term of (13) results from (8). Observe that, for a given SNR, the value of (14) is boosted by the term $1/T^2$. For instance, if SNR= $\frac{U^2}{2\sigma_\eta^2}$ = 60 dB, T = 20 ms, and M is in the order of 100, the square root of (13) (namely the standard uncertainty of $\delta_R\left(i^*\right)$) becomes 0.9 %/s. Therefore, the detection threshold $|R^*|$ should be at least about 4 %/s to keep the risk of false RVC detection low enough.

IV. Simulation-based performance comparison between RVC detection algorithms

In order to provide a detailed performance comparison between the IEC standard algorithm and the derivative-based approach described in Section III, multiple Monte Carlo simulations have been performed using 50-Hz voltage

waveforms sampled at 6.4 kHz (i.e. for $M = 128$) and affected by positive or negative RVCs with various relative amplitudes (i.e., $|\delta_U| = \{1\%, 2.5\%, 5\%, 7.5\%, 10\%\}$) and different rates of change of RMS voltage (i.e., $|R| = \{5\%, 10\ \%/s, 20\ \%/s, 50\ \%/s, 100\ \%/s, 200\ \%/s, 500\ \%/s, 1000\ \%/s\}$). Both sets of values refer to the ranges where RVCs clearly affect the flicker perception index defined in the IEC Standard 61000-4-15:2010 [31], as confirmed by the experiments reported in [1], [8]. The chosen values allow to analyze the behavior of either algorithm both in the case of minor, smooth events and when sudden, more severe RVCs occur. For each RVC, 256 values of parameters φ and t^* in (1) are changed randomly with a uniform probability density function within $[0,2\pi]$ and $[1, 1+T/2]$ seconds, respectively. To compare the behavior of RVC detection algorithms under realistic conditions, the SNR affecting the digitized waveform prior to RMS estimation is set to 60 dB. Moreover, 25 harmonics with random initial phase and amplitude equal to the maxima reported in the EN Standard 50160:2010 for Low-Voltage distribution systems are added to the fundamental tone [32]. The corresponding relative amplitudes are summarized below:

- **Even harmonics:** 2.0% (2nd harmonic), 1.0% (4th harmonic) and 0.5% (all the others till the 24th harmonic).
- **Odd harmonics multiples of 3:** 5.0% (3rd harmonic), 1.5% (9th harmonic) and 0.5% (15th and 21st harmonics);
- **Other odd harmonics:** 6.0% (5th harmonic), 5.0% (7th harmonic), 3.5% (11th harmonics), 3.0% (13th harmonics), 2.0% (17th harmonics), and 1.5% (19th, 23rd and 25th harmonics).

The resulting Total Harmonic Distortion (THD) is equal to 11.3% (i.e., larger than 8% as prescribed by the EN Standard 50160:2010 [32]). This value is large enough to compare the performances of both RVC detection algorithms under stressed operating conditions.

The respective RVC detection thresholds are set on the basis of the criteria explained in Section II.C and III.A, i.e. $S = 1\%$ or $S = 2\%$ for the IEC standard algorithm and $|R^*| = 4$ %/s for the derivative-based approach, respectively. For the sake of clarity, the actual and the estimated RMS voltages as well as the respective rates of change for an RVC with $\delta_U = -2.5\%$ and $R = -10$ %/s are shown in Fig. 4(a)-(b) along with the upper and lower detection thresholds of the IEC Standard algorithm (for $S = 1\%$) and the derivative-based approach (with $|R^*| = 4$ %/s).

Consider that the accuracy of both algorithms in measuring the RMS voltage is the same, as they both rely on the same estimator (7), whose accuracy has been already analyzed in [18] and [26]. Therefore, no further results on RMS voltage accuracy are reported in this paper. However, the two algorithms are expected to behave very differently in terms of detection latency, as qualitatively shown in Fig. 4 as well.

Tab. I shows the 99th percentiles of the RVC detection delays (expressed in nominal power line cycles) computed over 256 intervals and associated with either algorithm for different values of $|\delta_U|$ and $|R|$. Each detection delay results

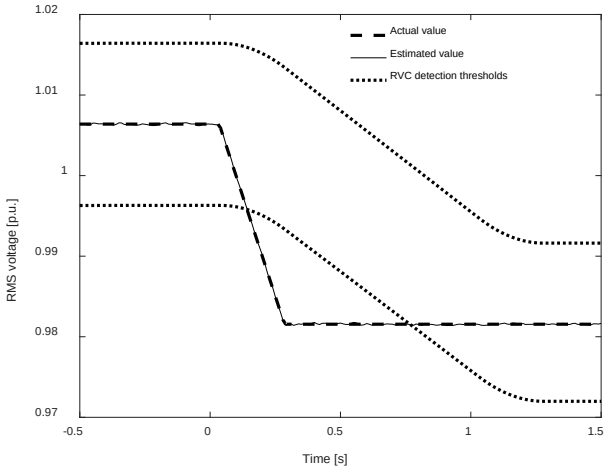

(a)

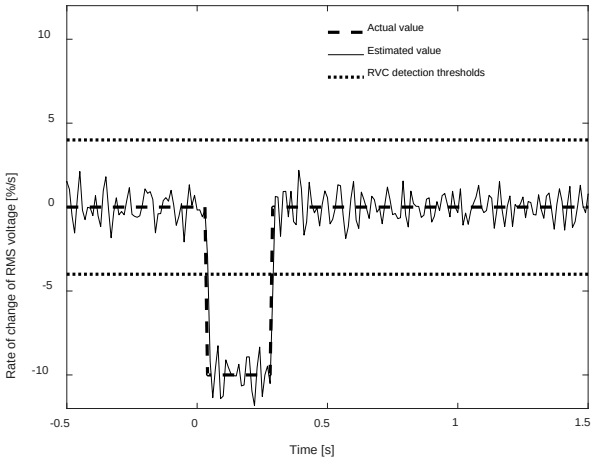

(b)

Fig. 4 – RMS voltage (a) and rate of change of RMS voltage (b) during an RVC with $\delta_U = -2.5\%$ and $R = -10$ %/s. Solid and dashed lines refer to estimated and actual values, respectively. The upper/lower detection thresholds (dotted lines) are based either on the IEC Standard algorithm for S=1% (a) or on the derivative-based approach for $|R^*| = 4$ %/s (b).

from the difference between the time at which the detection threshold of either algorithm is exceeded (corresponding to an integer multiple of a half power line cycle) and the instant when the RVC actually begins. Observe that using the IEC Standard algorithm some RVCs are never detected. This happens not only when $|\delta_U| < S$ (e.g., when $|\delta_U| = 1\%$ and $S = 2\%$), but also if the RVC rate of change is below the critical thresholds R_{m+} or R_{m-}. An example of this kind of situations occurs when $|\delta_U| = 2.5\%$, $|R| = 5$ %/s and $S = 2\%$. Indeed, in this case (4) and (5) return $|R_{m+}| \approx |R_{m-}| \approx 6$ %/s, and these limits are greater than $|R|$. Similarly, if $|\delta_U| = S = 1\%$, then $|R_{m+}| \approx |R_{m-}| \approx 100$ %/s. This explains why in this case only fast RVCs can be detected. From Tab. I, it is quite clear that the detection speed of the derivative-based approach is always faster than the IEC standard algorithm.

TABLE I – 99TH PERCENTILES OF DIFFERENT RVC DETECTION DELAYS (EXPRESSED IN NOMINAL POWER LINE CYCLES) OBTAINED WITH MONTE CARLO SIMULATIONS BY USING THE IEC STANDARD ALGORITHM FOR S=1% OR S=2%, AND THE DERIVATIVE-BASED APPROACH FOR $|R^*|$=4 %/S. ACRONYM *N.D.* STANDS FOR "NEVER DETECTED".

	$\|\delta_U\|$ = 1%			$\|\delta_U\|$ = 2.5%			$\|\delta_U\|$ = 5%			$\|\delta_U\|$ = 7.5%			$\|\delta_U\|$ = 10%		
$\|R\|$ [%/s]	***S*=1%**	***S*=2%**	**$\|R^*\|$=4 %/s**	***S*=1%**	***S*=2%**	**$\|R^*\|$=4 %/s**	***S*=1%**	***S*=2%**	**$\|R^*\|$=4 %/s**	***S*=1%**	***S*=2%**	**$\|R^*\|$=4 %/s**	***S*=1%**	***S*=2%**	**$\|R^*\|$=4 %/s**
5	*N.D.*	*N.D.*	2.0	12.6	*N.D.*	1.9	12.6	29.4	2.2	12.6	29.4	2.3	12.6	29.5	2.3
10	*N.D.*	*N.D.*	1.3	6.5	12.6	1.3	6.5	12.6	1.2	6.5	12.6	1.2	6.4	12.5	1.3
20	*N.D.*	*N.D.*	1.0	3.6	6.5	1.0	3.7	6.4	0.9	3.6	6.4	1.0	3.6	6.4	1.0
50	*N.D.*	*N.D.*	0.8	2.1	3.1	0.8	2.1	3.1	0.8	2.0	3.1	0.8	2.0	3.1	0.8
100	*N.D.*	*N.D.*	0.8	1.5	2.1	0.7	1.5	2.0	0.8	1.5	2.0	0.8	1.5	2.0	0.7
200	1.2.	*N.D.*	0.7	1.2	1.6	0.7	1.2	1.5	0.7	1.2	1.5	0.7	1.2	1.5	0.7
500	1.0.	*N.D.*	0.7	1.0	1.4	0.6	1.0	1.2	0.7	1.0	1.2	0.7	0.9	1.2	0.7
1000	1.0	*N.D.*	0.6	0.9	1.3	0.6	0.9	1.0	0.6	0.9	1.0	0.6	0.9	1.0	0.6

As expected, such a faster responsiveness is particularly significant when $|R|$ is small and it becomes even more evident if S grows. However, when the rate of change of RMS voltage increases and, consequently an RVC tends to become a sudden, step-like variation, the detection delays of both algorithms tend to the same minimum value, i.e. ½ cycle, in accordance with (6). Unfortunately, the derivative-based detection algorithm is also more sensitive to random contributions and noise, as expected from (14). For instance, if $|R^*|$ = 4 %/s and SNR = 60 dB, the probability of false RVC detection is about 0.06%, which is small, but not negligible. On the contrary, the standard algorithm with S = 1% or S = 2% is able to detect (although very slowly) RVCs with rates of change of RMS voltage so low as 6 %/s with a negligible probability of false detection.

The results in Tab. I also show that in all the cases considered, for given rates of change and thresholds, the detection delays are quite independent of the maximum relative voltage variation $|\delta_U|$. While this behavior is quite obvious for the derivative-based algorithm, it is less intuitive in the case of the standard one. However, this is consistent with (6), which indeed does not depend on δ_U.

The bar diagram in Fig. 5 shows the standard deviations of the rate of change estimates returned by the derivative-based algorithm as a function of $|R|$ for different voltage relative amplitude variations $|\delta_U|$. The results in Fig. 5 show that the uncertainty associated with the estimation of the rate of change of RMS voltage grows monotonically with $|R|$, but it depends weakly on $|\delta_U|$, unless fast RVCs (i.e. with $|R|$ in the order of hundreds of %/s) are considered. Indeed, when the derivative of the RMS voltage exhibits an impulsive shape, the accuracy of the backward Euler difference estimator over a half-cycle is quite poor.

To complete the analysis, the performances of the standard and the derivative-based RVC detection algorithms have been compared in the presence of RVCs exhibiting a time-varying rate of change of RMS voltage. To this purpose, the so-called "motor-start" RVC model has been adopted [8]. Due to the motor coil inductance, a sudden negative RMS voltage change occurs at motor start-up. Such a change is followed by an exponential ramp converging towards a new steady-state value [9]. Different RVCs based on the "motor-start" model have been generated by changing both the maximum RMS voltage amplitude variation (i.e., with δ_U = {-1%, -2.5%, -5%, -7.5%, -10%}) and the time constant τ of the following exponential ramp (i.e., with τ ranging between 2 ms and 200 ms). Again, the SNR is 60 dB and the THD is 11.3%. In addition, frequency deviations within ±0.5 Hz with 99.5% probability (i.e., compliant with [32]) have been included in simulations.

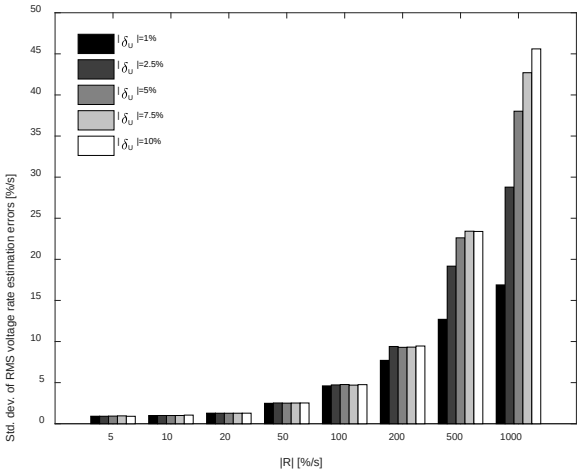

Fig. 5 – Standard deviation values of the RMS voltage rate of change estimation errors for RVCs of different magnitude and slope.

The actual and the estimated RMS voltage profiles of one "motor-start" RVC with δ_U = -7.5% and τ=100 ms, as well as the respective rates of change of RMS voltage are shown in Fig. 6(a)-(b). The upper and lower detection thresholds associated with the IEC Standard algorithm for S = 1% and those of the derivative-based approach for $|R^*|$ = 4 %/s are also plotted (dotted lines). However, the latter limits are hardly visible as they are much smaller than the maximum absolute rate of change. For this reason, the instant of detection is zoomed in the inlet of Fig. 6(b). The example in Fig. 6 just confirms that the derivative-based approach is able to detect the RVC, even if the RMS rate of change estimation accuracy is quite poor due to the sudden voltage variation, in accordance with the results of Fig. 5.

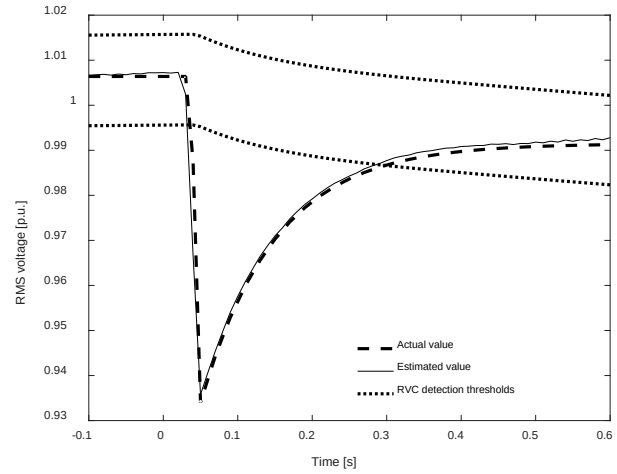

(a)

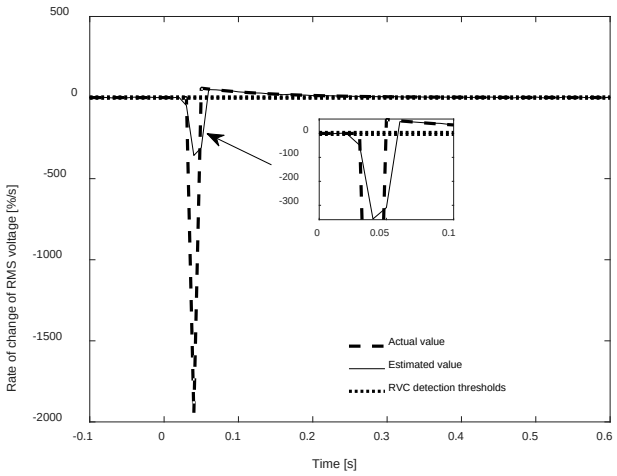

(b)

Fig. 6 – RMS voltage (a) and rate of change of RMS voltage (b) during an RVC corresponding to a "motor-start" event with δ_U = -7.5% and τ = 100 ms. Solid and dashed lines refer to estimated and actual values, respectively. The detection thresholds (dotted lines) are based either on the IEC Standard algorithm for S=1% (a) or on the derivative-based approach for $|R^*|$ = 4 %/s (b). In the latter case, the detection instant is zoomed in the inlet.

The results of other simulations obtained with "motor-start" RVCs of different amplitude are consistent with those shown in Fig. 6. Thus, they are not reported for the sake of brevity. Moreover, while the 99th percentiles of the detection delays obtained with the IEC standard algorithm range between about 0.7 and 1.1 power line cycles, the derivative-based approach ensures delays lower than about 0.5 cycles regardless of the values of δ_U and τ, thus confirming that the proposed alternative algorithm provides faster RVC detection.

V. Conclusion

The Rapid Voltage Change (RVC) detection limits and the related delays achievable with the algorithm described in the IEC Standard 61000-4-30:2015 depend not only on a specified fraction of the average RMS value, but also, quite unexpectedly, on the rate of change of the RMS voltage. As a result, RVCs that are not so fast could be hardly detected or could be detected only after tens of power line cycles even if measurement uncertainty is negligible. To address this problem, a simple algorithm based on the estimation of the rate of change (namely the derivative) of RMS voltage is proposed and characterized. Multiple simulation results show that the derivative-based detection algorithm is always faster than the standard one. However, this advantage is counterbalanced by larger sensitivity to noise and disturbances. For instance, if the Signal-to-Noise Ratio (SNR) of the digitized waveform is about 60 dB, RVCs with a rate of change or RMS voltage lower than about 5%/s could be hardly distinguished from fluctuations due to noise, regardless of RVCs amplitude.

This problem could be partially solved by using better estimators of the rate of change of RMS voltage or a hybrid approach. However, this aspect will be investigated in a future work.

Appendix A - Analytical Expression of $\overline{U}_{rms(1/2)}(i)$

With reference to signal model (1), let i be the time index corresponding to the zero-crossing of the current half-cycle and let L denote the half-cycle during which the RVC occurs. Without loss of generality, let us assume that the discretized duration of the RVC is shorter than 1 s, i.e. $K \leq N$-1 half-cycles, with N=100 or 120 depending on whether f=50 Hz or 60 Hz, respectively. Of course, if $i \leq L$ or $i > L+K+N$-1, then the RVC lies totally outside the moving average window. Thus, $\overline{U}_{rms(1/2)}(i) = \frac{U}{\sqrt{2}}$ and $\overline{U}_{rms(1/2)}(i) = \frac{U(1+\delta_U)}{\sqrt{2}}$, respectively. If $L < i \leq L+K$, then just the beginning of the RVC transient lies within the moving average window. Hence,

$$\overline{U}_{rms\,(1/2)}(i) = \frac{U}{N\sqrt{2}}\left\{L - i + N + \sum_{n=L+1}^{i}\frac{U}{\sqrt{2}}\left[1+\frac{RT}{2}(n-L)+R\tau_R\right]\right\} = \frac{U}{\sqrt{2}}\left\{1+\frac{RT}{2N}\sum_{n=L+1}^{i}(n-L)+R\tau_R\frac{i-L}{N}\right\} \quad \text{(A.1)}$$

where the summation on the rightmost side of (A.1) is a finite arithmetic series that can be calculated analytically. The corresponding result is indeed reported in the second row of (A.4).

If $L+K < i \leq L+N$-1, then the RVC transient is fully included in the moving average window. Thus,

$$\overline{U}_{rms\,(1/2)}(i) = \frac{U}{N\sqrt{2}}\left\{L - i + N + \sum_{n=L+1}^{L+K}\left[1+\frac{RT}{2}(n-L)+R\tau_R\right] + \sum_{n=L+K+1}^{i}(1+\delta_U)\right\} = \frac{U}{\sqrt{2}}\left\{1+\frac{RT}{2N}\sum_{n=L+1}^{L+K}(n-L)+R\tau_R\frac{K}{N}+\delta_U\frac{i-L-K}{N}\right\} \quad \text{(A.2)}$$

from which the third row of (A.4) results.

Finally, for $L+N$-1$< i \leq L+N$-1, just the ending part of the RVC transient lies within the moving average window. Therefore,

$$\overline{U}_{rms\,(1/2)}(i)=\frac{U}{N\sqrt{2}}\left\{\sum_{n=i-(N-1)}^{L+K}\left[1+\frac{RT}{2}(n-L)+R\tau_R\right]+\sum_{n=L+K+1}^{i}(1+\delta_U)\right\}$$

$$=\frac{U}{\sqrt{2}}\left\{1+\frac{RT}{2N}\sum_{n=i-(N-1)}^{L+K}(n-L)+R\tau_R\frac{K+L+N-i}{N}+\delta_U\frac{i-L-K}{N}\right\} \quad \text{(A.3)}$$

and the fourth row of (A.4) results.

APPENDIX B - DERIVATION OF (4) AND (5)

As explained in Section II.A, an RVC based on model (1) ideally ends during the (*L*+*K*)-th half-cycle, i.e. when $U_{rms(1/2)}(L+K)\cong U(1+\delta_U)$. Therefore, for given values of relative variation δ_U and rate of change *R*, the duration of an RVC expressed in number of half-cycles is given by $K=\frac{2\delta_U}{RT}-\frac{2\tau_R}{T}$. Assuming that *R* is unknown, by replacing first this expression of *K* into (3) and then both (3) and $U_{rms(1/2)}(L+K)\cong U(1+\delta_U)$ into (2), after some algebraic steps the following second-degree inequalities result, i.e.

$$-\tau_R T\left(1-\frac{2\tau_R}{T}\right)R^2+\left(\delta_U T+4\frac{(\delta_U-S)}{1+S}\right)R-2\delta_U^2\geq 0 \quad \text{(B.1)}$$

for *R*>0 and

$$-\tau_R T\left(1-\frac{2\tau_R}{T}\right)R^2+\left(\delta_U T+4\frac{(S+\delta_U)}{1-S}\right)R-2\delta_U^2\leq 0 \quad \text{(B.2)}$$

for *R*<0, respectively. In (B.1) and (B.2), *T* is expressed in seconds and *R* is expressed in s^{-1}. Of course, the analytical expressions of the minimum positive or maximum negative rates of change of RMS voltage for which a linear RVC is detected can be computed by solving (B.1) and (B.2). However, simpler, approximate expressions can be easily found by noticing that the second-degree terms of both (B.1) and (B.2) are quite negligible. Indeed, in borderline conditions for RVC detection, $R^2<R<<1\ s^{-1}$ (i.e. the rate of change is much smaller than 100 %/s). Moreover, given that τ_R is bounded in the interval [-*T*/2, *T*/2] with *T*=2/*N* (expressed in seconds), the coefficients of the second-degree terms lie within $[-T^2/8,\ T^2]$. Hence, they are in the order of 10^{-4}. Therefore, by neglecting $-\tau_R T\left(1-\frac{2\tau_R}{T}\right)R^2$ in (B.1) and (B.2), (4) and (5) immediately result.

APPENDIX C - DERIVATION OF (6)

Given expression (2), by replacing (A.1), $D=i^*-L$ and *T*=2/*N* seconds into (2), after a few algebraic steps, the following two second-degree equations result, i.e.

$$D^2-\frac{\frac{4}{T}+(1+S)\left(1-4\frac{\tau_R}{T}\right)}{1+S}D+\frac{\frac{8}{T^2}\left(\frac{S}{R}-\tau_R\right)}{1+S}=0 \quad \text{(C.1)}$$

for *R* > 0 and

$$D^2-\frac{\frac{4}{T}+(1-S)\left(1-4\frac{\tau_R}{T}\right)}{1-S}D-\frac{\frac{8}{T^2}\left(\frac{S}{R}+\tau_R\right)}{1-S}=0 \quad \text{(C.2)}$$

for *R*<0. Considering that in practice $(1\pm S)\left(1-4\frac{\tau_R}{T}\right)<<N=\frac{2}{T}$, the solutions of (C.1) and (C.2) are given approximately by

$$D=\frac{\frac{2}{T}+\frac{(1+S)}{2}\left(1-4\frac{\tau_R}{T}\right)}{1+S}\pm\frac{\Delta_+}{2}\approx\frac{2}{(1+S)T}\pm\frac{\sqrt{\Delta_+}}{2} \quad \text{(C.3)}$$

and

$$D=\frac{\frac{2}{T}+\frac{(1-S)}{2}\left(1-4\frac{\tau_R}{T}\right)}{1-S}\pm\frac{\Delta_-}{2}\approx\frac{2}{(1-S)T}\pm\frac{\sqrt{\Delta_-}}{2} \quad \text{(C.4)}$$

where

$$\Delta_+\approx\frac{\frac{16}{T^2}}{(1+S)^2}-\frac{\frac{32}{T^2}\left(\frac{S}{R}-\tau_R\right)}{(1+S)} \text{ and } \Delta_-\approx\frac{\frac{16}{T^2}}{(1-S)^2}+\frac{\frac{32}{T^2}\left(\frac{S}{R}+\tau_R\right)}{(1-S)} \quad \text{(C.5)}$$

for *R* > 0 and *R* < 0, respectively.

$$\overline{U}_{rms\,(1/2)}(i)=\begin{cases}\frac{U}{\sqrt{2}} & i\leq L\\ \frac{U}{\sqrt{2}}\left\{1+\frac{RT}{4N}(i-L)(i-L-1)+\frac{i-L}{N}R\tau_R\right\} & L<i\leq L+K\\ \frac{U}{\sqrt{2}}\left\{1+\frac{RT}{4N}K(K-1)+\frac{i-L-K}{N}\delta_U+\frac{K}{N}R\tau_R\right\} & L+K<i\leq L+N-1\\ \frac{U}{\sqrt{2}}\left\{1+\frac{RT}{4N}\left[K(K-1)-(i-L-N)(i-L-N-1)\right]+\frac{i-L-K}{N}\delta_U+\frac{L+K+N-i}{N}R\tau_R\right\} & L+N-1<i\leq L+K+N-1\\ \frac{U}{\sqrt{2}}(1+\delta_U) & i>L+K+N-1\end{cases} \quad \text{(A.4)}$$

Of course, the solutions of (C.3) and (C.4) have a physical meaning if and only if:

1. the roots of (C.1) and (C.2) are real-valued (namely if $\Delta_+ \geq 0$ and $\Delta_- \geq 0$);
2. the smaller roots of (C.3) and (C.4) range between 0 and K.

The former condition is certainly conservatively met if (4) and (5) hold. The latter instead is intuitively justified by the fact that i) D must be a positive quantity and ii) if condition (2) does not hold for $i^* = L+K$ (or equivalently for $D = K$), then an RVC cannot be detected for the reasons explained in Section II.A. Observe that the smaller roots of (C.3) and (C.4) reach their maxima for $\tau_R=T/2$ and $\tau_R=-T/2$, respectively. Therefore, by rounding such solutions to the closest larger integer value, (6) finally results.

REFERENCES

[1] J. Barros, M. de Apráiz, R. I. Diego, J. J. Gutiérrez, P. Saiz and I. Azcarate, "Minimum requirements for rapid voltage changes regulation based on their effect on flicker," Proc. *IEEE International Workshop on Applied Measurements for Power Systems (AMPS)*, Liverpool, UK, 2017, pp. 1-5.

[2] J. Barros, J. J. Gutiérrez, M. de Apráiz, P. Saiz, R. I. Diego and A. Lazkano, "Rapid Voltage Changes in Power System Networks and Their Effect on Flicker," *IEEE Trans. on Power Delivery*, vol. 31, no. 1, pp. 262-270, Feb. 2016.

[3] A. J. Schlabbach, D. Blume, T. Stephanblome, *Voltage quality in electrical power systems*, Institution of Electrical Engineers, London, 2001.

[4] M. H. J. Bollen, M. Häger, and C. Schwaegerl, "Quantifying voltage variations on a time scales between 3 seconds and 10 minutes," Proc. 18th Int. Conf. Elect. Distrib, Turin, Italy, 2005.

[5] V. Agarwal, L. H. Tsoukalas, "Smart grids: importance of Power Quality," in *Energy-Efficient Computing and Networking* (N. Hatziargyriou, A Dimeas, T: Tomtsi, A. Weidlich, Editors), pp. 136-143, Springer, Berlin-Heidelberg, 2011.

[6] IEEE Std. 1159:2009, *IEEE Recommended Practice for Monitoring Electric Power Quality*, Jun. 2009.

[7] *IEEE P1159.3/D18, IEEE Draft Recommended Practice for Power Quality Data Interchange Format (PQDIF)*, Jan. 2018.

[8] K. Brekke, H. Seljeseth, and O. Mogstad "Rapid voltage changes - definition and minimum requirements," *IET Conference Proceedings*, Prague, Czech Republic, Jun. 2009, p. 789-789.

[9] IEC Std. 61000-4-30:2015, *Electromagnetic Compatibility (EMC) – Part 4-30: Testing and measurement techniques – Power Quality Measurement Methods*, Feb. 2015.

[10] Chau-Shing Wang and M. J. Devaney, "Incandescent lamp flicker mitigation and measurement," *IEEE Trans. Instr. and Meas.*, vol. 53, no. 4, pp. 1028-1034, Aug. 2004.

[11] G. Bucci, E. Fiorucci and F. Ciancetta, "The Performance Evaluation of IEC Flicker Meters in Realistic Conditions," *IEEE Trans. Instr. and Meas.*, vol. 57, no. 11, pp. 2443-2449, Nov. 2008.

[12] X. X. Yang and M. Kratz, "Power System Flicker Analysis by RMS Voltage Values and Numeric Flicker Meter Emulation," *IEEE Trans. on Power Delivery*, vol. 24, no. 3, pp. 1310-1318, Jul. 2009.

[13] R. Iuzzolino and W. G. K. Ihlenfeld, "High-Accuracy Methods and Measurement Procedures for Power Quality Parameters Using the Digital Synchronous Sampling Technique," *IEEE Trans. Instr. and Meas.*, vol. 56, no. 2, pp. 426-430, Apr. 2007.

[14] N. Locci, C. Muscas and S. Sulis, "On the Measurement of Power-Quality Indexes for Harmonic Distortion in the Presence of Capacitors," *IEEE Trans. Instr. and Meas.*, vol. 56, no. 5, pp. 1871-1876, Oct. 2007.

[15] D. Gallo, C. Landi, M. Luiso and E. Fiorucci, "Survey on Voltage Dip Measurements in Standard Framework," *IEEE Trans. Instr. and Meas.*, vol. 63, no. 2, pp. 374-387, Feb. 2014.

[16] A. Moschitta, P. Carbone, C. Muscas, "Generalized Likelihood Ratio Test for Voltage Dip Detection," *IEEE Trans. Instr. and Meas.*, vol. 60, no. 5, pp. 1644-1653, May 2011.

[17] S. Rinaldi, D. Della Giustina, P. Ferrari, A. Flammini, "Distributed monitoring system for voltage dip classification over distribution grid", Sustainable Energy, Grids and Networks, Vol. 6, pp. 70-80, Jun. 2016.

[18] J. Barros, P. Saiz, M. de Apráiz, L. A. Leturiondo, R. I. Diego and J. J. Gutiérrez, "Limitations in the use of the IEC standard method for detection and analysis of rapid voltage changes in power system networks," Proc. *International Conference on Harmonics and Quality of Power (ICHQP)*, Belo Horizonte, Brazil, Dec. 2016, pp. 530-534.

[19] D. Macii and D. Petri, "Fast detection of rapid voltage change events through dynamic RMS voltage tracking," Proc. *IEEE International Instrumentation and Measurement Technology Conference* (I^2MTC), Houston, TX, USA, May 2018, pp. 1-6.

[20] A. F. Bastos, K. Lao, G. Todeschini and S. Santoso, "Novel Moving Average Filter for Detecting RMS Voltage Step Changes in Triggerless PQ Data," in *IEEE Transactions on Power Delivery*, vol. 33, no. 6, pp. 2920-2929, Dec. 2018.

[21] D. Macii, D. Fontanelli and D. Petri, "Performance of Phasor Measurement Units for power quality event detection in urban distribution grids," Proc. *IEEE International Smart Cities Conference* (ISC2), Trento, Italy, Sep. 2016, pp. 1-7.

[22] A. M. Dumitrescu, R. Roman and M. Albu, "Synchronized measurements and power quality assesment," Proc. *IEEE PowerTech*, Eindhoven, Netherlands, Jun.-Jul. 2015, pp. 1-6.

[23] S. Kumar, M. K. Soni and D. K. Jain, "Power Quality Monitoring using PMU," *International Journal of Computer Applications*, vol. 135, no. 7, pp. 1-5, Feb. 2016.

[24] A. R. Toma, A. M. Dumitrescu and M. Albu, "Assessment of rapid voltage changes using PMU data," *IEEE International Workshop on Applied Measurements for Power Systems (AMPS)*, Aachen, Germany, 2015, pp. 126-131.

[25] A. R. Toma, A. M. Dumitrescu and M. Albu, "Impact of measurement set-up on RVC-like event detection," Proc. *IEEE Int. Instr. and Meas. Tech. Conf.* (I^2MTC), Taipei, Taiwan, May 2016, pp. 1-5.

[26] D. Macii, D. Petri, "On the detection of Rapid Voltage Change (RVC) events for power quality monitoring," Proc. *IEEE Int. Instr. and Meas. Tech. Conf.* (I^2MTC), Turin, Italy, May 2017, pp. 1-6.

[27] M. Bertocco, C. Narduzzi, P. Paglierani and D. Petri, "A noise model for digitized data," in *IEEE Transactions on Instrumentation and Measurement*, vol. 49, no. 1, pp. 83-86, Feb. 2000.

[28] D. Macii, D. Fontanelli, G. Barchi and D. Petri, "Impact of Acquisition Wideband Noise on Synchrophasor Measurements: A Design Perspective," in *IEEE Transactions on Instrumentation and Measurement*, vol. 65, no. 10, pp. 2244-2253, Oct. 2016.

[29] D. Macii, L. Mari and D. Petri, "Comparison of Measured Quantity Value Estimators in Nonlinear Models," in *IEEE Transactions on Instrumentation and Measurement*, vol. 59, no. 1, pp. 238-246, Jan. 2010.

[30] M. Luiso, D. Macii, P. Tosato, D. Brunelli, D. Gallo and C. Landi, "A Low-Voltage Measurement Testbed for Metrological Characterization of Algorithms for Phasor Measurement Units," in *IEEE Transactions on Instrumentation and Measurement*, vol. 67, no. 10, pp. 2420-2433, Oct. 2018.

[31] IEC 61000-4-15:2010, *Electromagnetic Compatibility (EMC) – Part 4-15: Testing and measurement techniques. Flickermeter, Functional and design specifications*, Aug. 2010.

[32] EN 50160:2010, *Voltage characteristics of electricity supplied by public distribution systems*, Brussels, Belgium, Dec. 2010.